Surface Albedo Feedback Estimates for the AR4 Climate Models

Michael Winton

Geophysical Fluid Dynamics Laboratory/NOAA

Revised for *Journal of Climate*

26 July 2005

Corresponding author: Dr. Michael Winton, GFDL/NOAA, P.O. Box 308, Princeton University Forrestal Campus, Princeton, NJ 08542. email: Michael.Winton@noaa.gov

Abstract

A technique for estimating surface albedo feedback (SAF) from standard monthly mean climate model diagnostics is applied to the 1%/year CO_2 increase transient climate change integrations of twelve IPCC AR4 climate models. Over the 80 year runs, the models produce a mean SAF at the surface of 0.3 $Wm^{-2}K^{-1}$ with a standard deviation of 0.09 $Wm^{-2}K^{-1}$. Compared to $2xCO_2$ equilibrium run estimates from an earlier group of models, both the mean SAF and the standard deviation are reduced. Three quarters of the model mean SAF comes from the northern hemisphere in roughly equal parts from the land and ocean areas. The remainder is due to southern hemisphere ocean areas. The SAF differences between the models are shown to stem mainly from the sensitivity of the surface albedo to surface temperature rather from the impact of a given surface albedo change on the shortwave budget.

I. Introduction

Surface albedo feedback is a mechanism that enhances climate change, particularly in regions with snow and ice cover. As the earth warms (cools), the surface reflects less (more) shortwave radiation to space due to changes in the coverage and reflectivity of the surface ice cover, which contribute additional warming (cooling) – a positive feedback. The surface albedo feedback (SAF) is conventionally defined as the change in net shortwave flux, S, due to the impact of a change in surface temperature, T_S, upon surface albedo, α_S:

$$SAF = \frac{\partial S}{\partial \alpha_S}\frac{\partial \alpha_S}{\partial T_S} \qquad (1)$$

The SAF may be defined at the top-of-atmosphere or at the surface – the difference being due to changes in atmospheric absorption of surface reflected shortwave. The SAF and other feedbacks, f_i, are useful for diagnosing the causes of the sensitivity of the global mean surface temperature to a given forcing, F, using a zero-dimensional energy balance model:

$$\Delta T_S = -F \Big/ \sum f_i \qquad (2)$$

The dominant feedback is negative and due to increased outgoing longwave radiation with increased temperature. The water vapor feedback and SAF are positive feedbacks, contributing to an increased temperature change for a given forcing by countering the temperature feedback and reducing the magnitude of the denominator.

The role of SAF in CO_2 doubling induced climate change has been investigated by Hall (2004) using the GFDL climate model. Hall found that suppressing the SAF reduced the warming at the North Pole from 5 K to 2 K above the equatorial warming. The impact of SAF was largest at the poles but extended all the way to the equator. Hall studied the climate impact of SAF in the GFDL model but did not quantify it. The standard technique for quantifying a climate model's SAF involves running an offline shortwave radiation calculation with the same inputs as the online calculation but swapping the control surface albedo (α_S) and the

perturbation run surface albedo (α_S') to determine the change in shortwave fluxes. Dividing this change by the change in surface temperature gives an estimate of (1):

$$SAF \approx \frac{\Delta S_{\alpha_S \rightarrow \alpha_{S'}}}{\Delta T_S} \qquad (3)$$

A number of factors beside surface temperature, typically taken to be surface *air* temperature, also affect the surface albedo. Snowfall and sea surface temperature are two prominent examples. Nonetheless, it is common to interpret the modeled relationship between surface albedo induced shortwave flux and surface temperature change obtained by comparing a control and perturbation experiment as an estimate of SAF. In principle, a global average SAF could be constructed by time and space averaging (3) directly. However averaging the numerator and denominator separately and then taking the ratio yields a quantity that is more useful for global climate sensitivity analyses because the variables in such analyses are indexed to global mean surface air temperature (eqn. 2).

Model estimates of SAF have been made using atmospheric models forced with increased SSTs (Cess et al 1991) and with equilibrium $2xCO_2$ experiments performed with atmosphere-mixed-layer-ocean models (Colman 2003). The first method can only estimate SAF over land where surface conditions are allowed to vary. Colman (2003) has collected estimates made using the second method for twelve climate models. This ensemble had a mean top-of-atmosphere SAF of 0.36 $Wm^{-2}K^{-1}$ with a standard deviation of 0.19 $Wm^{-2}K^{-1}$. This was somewhat smaller than the models' mean cloud feedback of 0.55 $Wm^{-2}K^{-1}$ and considerably smaller than their mean water vapor feedback of 1.7 $Wm^{-2}K^{-1}$.

Just as the transient or *effective* sensitivity of a climate model may differ from its equilibrium sensitivity (see IPCC 2001, Chapter 9, Table 1), a transient feedback may also be different than an equilibrium feedback and may vary along the approach to equilibrium (Murphy, 1995). It is desirable to calculate the surface albedo feedback from transient experiments rather than equilibrium experiments for two reasons:

(1) The climate models used for transient experiments employ the full dynamic ocean components that are necessary to properly represent ocean/sea ice interactions (e.g. Winton 2003). The impact of warming-induced hydrologic cycle intensification on ocean circulation and mixing is not present in the atmosphere-slab ocean models used for $2xCO_2$ equilibrium experiments, for example.

(2) To the extent that the transient and equilibrium SAFs are different, the transient SAF is more relevant to the earth's future climate under the influence of anthropogenic greenhouse gases.

Although not a dominant player in the global climate sensitivity of a model, the SAF has outsized importance for snow- and ice-covered regions. The high-latitude response to increased CO_2 is quite variable amongst climate models (Holland and Bitz 2003). Holland and Bitz identify a number of processes that contribute to the polar amplification and its variation in climate models. Quantifying and understanding the contribution of SAF to differences among the models is a step toward reducing the uncertainty in projections of climate change in high-latitude and high-altitude ice covered regions.

In this study a new technique for calculating the SAF based on standard monthly-mean model diagnostics (Winton 2005) is applied to the global climate model simulations that have been performed to support the fourth assessment report (AR4) of the IPCC. Although a large suite of common experiments have been made and archived for the AR4, for purposes of comparability, the analysis in this paper makes use of 80 year averages of the 1%/year CO_2 increase to doubling experiments and the companion control experiments of twelve of the participating models (Table 1). The next section describes the method to be used to calculate SAF and tests it against a more accurate technique using the GFDL model. The third section presents the results from applying the method to the AR4 models. The results are summarized in the final section.

II. The Method

The offline radiative calculation that is needed to calculate the SAF has typically been made with a model's full radiation code – a very cumbersome procedure that entails saving all of the radiatively active quantities at high frequency and feeding them back into the offline radiation program. Winton (2005) explored techniques for simplifying this calculation by using simple optical models, fit to the climate model's monthly shortwave radiation diagnostics, for the offline calculation. After fitting, only the control and perturbation monthly surface albedos need be supplied to these models to estimate the numerator in the equation 3 SAF approximation.

Winton (2005) developed several such simple optical models. The most accurate of these is a 4-parameter method that fits upward and downward atmospheric albedos and transmissivities. Winton showed that this model, using monthly mean diagnostics, could estimate surface absorption over a large range of surface albedos with an RMS error of less than 2%. Unfortunately, the 4-parameter technique requires two extra diagnostics that are not currently available for the models: the surface downward and top-of-atmosphere upward shortwave fluxes over a zero-albedo surface. However, another technique, the ALL/CLR method, with a somewhat larger error (about 3% RMS surface absorption error) can be used to estimate the impact of a surface albedo change on the surface shortwave budget using existing diagnostics. The name "ALL/CLR" refers to the the all-sky/clear-sky surface downward shortwave ratio used in the parameterization (see below). Unlike the 4-parameter technique, which estimates both top of atmosphere and surface flux changes, the ALL/CLR technique is restricted to the surface. This is not a major restriction because the impact of surface albedo on the top of atmosphere budget is typically reduced by less than 10% from its impact on the surface budget according to results using the GFDL AM2 model (Winton 2005). The closeness of the surface and top-of-atmosphere SAF is due to the small impact of compensating atmospheric absorption over high-latitude and high-altitude icy regions.

Because an accurate treatment of multiple cloud-ground reflections is key, the ALL/CLR method hinges upon an estimate of the reflectivity of the atmosphere to shortwave radiation propagating upward from the surface, $\alpha_{\uparrow}$. The upward atmospheric reflectivity is parameterized as

$$\alpha_{\uparrow} = 0.05 + 0.85\left(1 - S_{B\downarrow} / S_{B\downarrow CLR}\right). \quad (4)$$

Where $S_{B\downarrow}$ and $S_{B\downarrow CLR}$ are the downward shortwave at the surface under all skies and clear skies. This reflectivity is mainly due to reflections from the undersides of clouds and will depend upon cloud parameters such as cloud water path and effective drop radius. The coefficients in eqn. 4 are round numbers based on physical reasoning and not fit to any particular model result (Winton 2005). Once $\alpha_{\uparrow}$ is calculated, the surface shortwave absorption, S_B ($\equiv S_{B\downarrow} - S_{B\uparrow}$), from standard scattering layer adding methods (e.g. Petty 2004), is

$$S_B(S_{B\downarrow}, S_{B\uparrow}, \alpha_{\uparrow}, \alpha_S) = S_{B\downarrow}\left(1 - \alpha_S\right)\left(1 - \alpha_{\uparrow} S_{B\uparrow} / S_{B\downarrow}\right) / \left(1 - \alpha_{\uparrow}\alpha_S\right). \quad (5)$$

To demonstrate its suitability for the present study, the ALL/CLR technique was tested in an equilibrium $2xCO_2$ experiment of GFDL's AM2 based slab mixed layer model. This code was instrumented to obtain the 4-parameter estimates for comparison. Figure 1 shows the impact of perturbing atmospheric (A->A', vertical arrows) and surface (S->S', horizontal arrows) optical properties on the surface and, for the 4-parameter technique, the atmospheric shortwave budget. Of course, the effect of perturbing both surface and atmospheric optical properties at once (the diagonal arrows) is available without using an auxiliary model.

It is evident from comparing the values on the upper and lower horizontal arrows that the sensitivity of the surface budget to surface albedo is significantly different (about 15%) for the control and perturbed atmosphere. This reflects the nonlinearity of shortwave processes. In this case, the $2xCO_2$ atmosphere allows less shortwave through to icy surfaces and so has a reduced sensitivity to surface albedo changes. To account for this we take the average of the two estimates, so for our ALL/CLR SAF estimates we will use:

$$\Delta S_{\alpha_S \to \alpha_S'} = \frac{S_B(S_{B\downarrow}, S_{B\uparrow}, \alpha_\uparrow, \alpha_S') - S_B(S_{B\downarrow}, S_{B\uparrow}, \alpha_\uparrow, \alpha_S) + S_B(S_{B\downarrow}', S_{B\uparrow}', \alpha_\uparrow', \alpha_S') - S_B(S_{B\downarrow}', S_{B\uparrow}', \alpha_\uparrow', \alpha_S)}{2} \quad (6)$$

Where primed quantities are obtained from the perturbation experiment monthly mean diagnostics and unprimed quantities from the control experiment.

Comparing the surface and atmospheric shortwave budget changes due to altering the surface albedo in Figure 1, it is apparent that the atmospheric absorption change is opposite the surface absorption change but of less than 10% of its magnitude. Winton (2005) shows that this is mainly due to the low absorptivity of the atmosphere to upward propagating shortwave in high-latitude and high-altitude regions. For this reason, the lack of information about atmospheric absorption sensitivity to surface albedo does not appear to be a critical problem for the ALL/CLR method. The top-of-atmosphere albedo sensitivity, the sum of the surface and atmospheric sensitivities, will be similar to the surface sensitivity but slightly reduced by atmospheric compensation. Of course it would be useful to check for the weakness of atmospheric compensation in models other than the GFDL model. In agreement with the more general results of Winton (2005), the ALL/CLR estimates of surface albedo sensitivities are fairly close to those of the more accurate and well-founded 4-parameter method for the $2xCO_2$ experiment shown in Fig. 1.

III. Results

Figure 2 shows the surface air temperature change, SAF, and the surface albedo temperature sensitivity ($\Delta\alpha_S/\Delta T_S$) averaged over years 1 to 80 of the 1%/year CO_2 increase experiments and then averaged over the twelve AR4 models used for this study. The SAF has been calculated using the ALL/CLR method described in the last section. The branch point from the control was determined as documented for models providing documentation and guessed from time and global temperature data for the others. All models are branched from a pre-industrial control experiment except the NCAR CCSM3.0 which is branched from a present day control experiment. The GISS model uses a different method than the others for estimating the clear-sky

shortwave – only recording a value when clear skies are found. This should not have a large impact on the SAF estimate. Monthly mean shortwave diagnostics are used in equations 4 and 5 to make the SAF estimates.

The lower two panels of Figure 2 show the *local* contribution to the *global* SAF and albedo temperature sensitivity – that is, they are the local changes, ΔS and $\Delta\alpha_S$, divided by the *global* surface air temperature change. Normalizing with the local temperature would give an estimate of the local SAF. This can lead to very large values in places where the temperature change is small. The technique of using global temperature change for local normalization has been used in a study of climate sensitivity by Boer and Yu (2003).

Figure 2b shows large contributions to SAF over the Himalaya, at the northern hemisphere sea ice edge and in Hudson's Bay. Smaller values are broadly distributed over the interior of the northern hemisphere continents, the Arctic sea ice and the southern hemisphere sea ice. The ice sheets make very little contribution. Presumably, the warming in the experiments is insufficient to bring significant fractions of the ice sheets near melting temperatures where surface albedo would be reduced. Land areas, southern hemisphere oceans and northern hemisphere oceans account for 39%, 37%, and 24% of the global SAF, respectively. Because SAF is so small over Antarctica and other southern hemisphere land masses, the land SAF contributes almost entirely to the Northern Hemisphere. Thus, the Northern Hemisphere contributes about ¾ of the global SAF.

Figure 2a shows a familiar pattern of CO_2 induced temperature change with relatively larger values over land and over the Arctic and warming minima in the Southern ocean and subpolar North Atlantic. The warming pattern and the SAF pattern are uncorrelated in the southern hemisphere but show significant similarities in the Northern Hemisphere in the sea ice regions and the mountain regions of the Asian and North American continents. The surface albedo temperature sensitivity (Fig. 2c) is quite similar to the SAF but with less emphasis in the relatively low latitude land regions where larger top-of-atmosphere insolation increases the contribution to SAF.

Table 1 lists the models with their surface air temperature changes and their global SAFs. The SAFs are broken down into land and hemispheric ocean contributions. Relative to its mean contribution the southern hemisphere ocean is the most variable of the three regions. More than half of the models have significant regions of negative SAF contribution in their Southern Oceans (not shown) and one model has an overall negative contribution in the region. Negative SAF contributions are possible where surface albedo increases in spite of global warming. This can occur, for example, in places where increased ocean halocline stratification due to intensification of the global hydrologic cycle leads to reduced ocean heat flux, local cooling, and an increase in sea ice.

The 80-year averaging places the time of the Table 1 estimates at 40 years from the beginning of the experiment. A more conventional analysis time period for 1%/year CO_2 increase experiments is the twenty year interval centered on year 70 (the time of doubling). The Table 1 numbers have also been calculated for this period (not shown). The global and regional SAF numbers are changed less than 7% when using this alternative averaging interval. This indicates a fair degree of temporal stability of the estimates.

Compared to the ensemble of models collected by Colman (2003), the current group's global mean SAF of 0.30 $Wm^{-2}K^{-1}$ is 17% less and its standard deviation of 0.09 $Wm^{-2}K^{-1}$ is about 50% less. As mentioned earlier, the numbers presented here are for the surface rather than the top-of-atmosphere as in Colman's study but experience with the GFDL model suggests that this should account for only about 10% of the reduction in mean and standard deviation. Another factor in the SAF reduction may be slowing of sea ice retreat in transient experiments due to increased atmospheric poleward water transport leading to reduced sea surface salinity and increased ocean stratification. Ice can be retained in such regions longer because of the reduction in ocean heat flux to the surface. Murphy (1995) documents such a suppression of the surface albedo feedback in a transient experiment with the Hadley Centre model. This hydrologic cycle impact is absent in

the equilibrium $2xCO_2$ experiments which make use of simple ocean mixed layer models. Finally, the current group of models are of a later vintage, having no model in common with the Colman group.

Over the course of the 80 year runs the numerator and denominator of (3) tend to be highly correlated. Global pentadal means of ΔS and ΔT_S are correlated at 0.85 or higher in ten of the twelve models. Among the models, the 80 year-averaged ΔS and ΔT_S have a correlation of 0.87. Hence the SAF is reasonably stable for the individual models and a useful way to characterize their differences.

The 80 year mean SAF itself is also moderately correlated (r=0.59) with the 80 year mean ΔT_S across the models. Some relationship is expected since SAF contributes to a model's sensitivity. The nonlinear way that feedbacks combine to make a model's sensitivity makes it difficult to gauge the contribution of the SAF to the intermodel transient climate sensitivity differences without knowing the other feedbacks (see eqn. 2). Since SAF is generally small compared to the other feedbacks, it is most likely to contribute substantially to the sensitivity when the sum of the other feedbacks approaches the value of the surface temperature feedback, the largest negative feedback (about 3.3 $Wm^{-2}K^{-1}$). When this happens the total feedback approaches zero and the response becomes large. Colman (2003) estimates, taking the other feedbacks at their mean values, that the standard deviation of 0.19 $Wm^{-2}K^{-1}$ for the models' SAF leads to a range of 1.3K in equilibrium $2xCO_2$ sensitivity. In the context of a transient experiment, the uncertainty introduced by SAF differences may be further reduced due to correlation of model sensitivity and ocean heat uptake (Raper et al 2002).

The land and northern hemisphere ocean contributions to SAF listed in Table 1 are only weakly correlated to each other (r=0.28) and virtually uncorrelated with the southern hemisphere ocean contribution ($|r|<0.07$). The same is true for regional SAFs constructed by using regional temperature change averages in the denominator of (2). These facts imply that each model can usefully be thought of as having three quasi-independent SAFs operating in the three regions. This contrasts with the temperature changes in the three

regions which are well correlated. There may also be independent regions within these three broad regions but a detailed geographic picture of the model SAF contribution differences is beyond the scope of this study.

Another way to break down the SAF differences between the models is to examine the roles of the two factors in its definition (eqn. 1). The first factor will be strongly influenced by atmospheric properties and by the meridional distribution of ice through its influence on top-of-atmosphere insolation. The second factor is more closely related to the surface state and the processes that control it. To assess the individual roles of the two terms we construct an estimate of the second factor, the albedo-temperature sensitivity:

$$\frac{\partial \alpha_S}{\partial T_S} \approx \frac{\Delta \alpha_S}{\Delta T_S} \qquad (7)$$

Since $\Delta\alpha_S$ is the change of a ratio we have the choice of direct or effective (separate numerator/denominator) averaging. Effective averaging can introduce atmospheric effects through weighting differences due to cloud shielding, for example. In order to gather such atmospheric effects in the first SAF factor, direct averaging of the local effective albedo is used. There is no viable alternative to using the local effective albedo since the seasonal variation of insolation is too large to make a direct time average of the local surface albedo sensible.

The SAF and equation 7 estimates of $\partial \alpha_S / \partial T_S$ for the models globally and for the three regions are scatter plotted in Figure 3. The albedo-temperature sensitivity and SAF are well correlated in all three regions. The correlation is particularly strong in the southern hemisphere oceans. This suggests that surface processes are playing a large role in the SAF differences between the models. Figure 3 also shows that the lower value of southern hemisphere ocean SAF relative to the other regions is associated with a correspondingly lower regional surface albedo-temperature sensitivity. The line in Figure 3 has a slope equal to the model mean global $\Delta S/\Delta\alpha_S$. This slope gives an estimate for the first factor in the SAF definition (eqn. 1) of 0.9 Wm^{-2} increased surface shortwave absorption for a 0.01 reduction in surface albedo.

IV. Conclusions

In this study a technique for calculating the surface albedo feedback has been tested and applied to transient CO_2 warming simulations of twelve climate models participating in the IPCC AR4. The models have a mean value of 0.3 $Wm^{-2}K^{-1}$ and a standard deviation of 0.09 $Wm^{-2}K^{-1}$. These numbers are comparable but somewhat smaller than earlier estimates from equilibrium $2xCO_2$ runs. The lack of correlation between the model values for land and the two hemispheric ocean regions suggests that, to resolve differences in the models' SAFs, regional differences will have to be considered separately. Breaking down the SAF into atmospheric and surface components points to the importance of the latter for the model differences. These results suggest that future work should focus on the regional snow and sea ice interactions with local temperature changes to try to account for the differences in surface albedo feedback. Although the surface albedo feedback is generally smaller than the water vapor feedback and less variable than cloud feedbacks, it is strongly associated with local temperature changes in the Northern Hemisphere. Therefore it provides a potential pathway to understanding climate change on a smaller scale.

Acknowledgements: The author thanks Keith Dixon, Tony Beesley and two anonymous reviewers for their helpful comments on the manuscript. The author also acknowledges the international modeling groups for providing their data for analysis, the Program for Climate Model Diagnosis and Intercomparison (PCMDI) for collecting and archiving the model data, the JSC/CLIVAR Working Group on Coupled Modelling (WGCM) and their Coupled Model Intercomparison Project (CMIP) and Climate Simulation Panel for organizing the model data analysis activity, and the IPCC WG1 TSU for technical support. The IPCC Data Archive at Lawrence Livermore National Laboratory is supported by the Office of Science, U.S. Department of Energy.

References

Boer, G.J., and B. Yu, 2003: Climate sensitivity and response, *Climate Dynamics*, **20**, 415—429.

Cess, R.D., G.L. Potter, J.P. Blanchet, G.J. Boer, R. Colman, S.J. Ghan, J. Hansen, J.T. Kiehl, H. Le Treut, Z-X Li, B.J. McAvaney, V.P. Meleshko, J.F.B Mitchell, J-J Morcrette, D.A. Randall, L.J. Rikus, E. Roeckner, U. Schlese, D.A. Sheinin, A. Slingo, A.P. Sokolov, K.E. Taylor, W.M. Washington, R.T. Wetherald, and I Yagaii, 1991: Intercomparison and interpretation of snow-climate feedback processes in nineteen atmospheric general circulation models, *Science*, **253**, 888—892.

Colman, R., 2003: A comparison of climate feedbacks in general circulation models, *Clim. Dyn.*, **20**, 865—873.

Hall, A., 2004: The role of surface albedo feedback in climate, *J. Climate*, **17**, 1550--1568.

Holland, M.M., and C.M. Bitz, 2003: Polar amplification of climate change in coupled models, *Climate Dynamics*, **21**, 221--232.

IPCC, 2001: Climate Change 2001: The scientific basis. Cambridge University Press, 881 pp.

Murphy, J.M., 1995: Transient response of the Hadley Centre coupled ocean-atmosphere model to increasing carbon dioxide: Part III analysis of global-mean response using simple models, *J. Climate*, **8**, 57—80.

Petty, G. W., 2004: A first course in atmospheric radiation. Sundog Publishing, 444 pp.

Raper, S.C.B., J.M. Gregory, and R.J. Stouffer, 2002: The role of climate sensitivity and ocean heat uptake on AOGCM transient temperature response, *J. Climate*, **15**, 124—130.

Winton, M., 2005: Simple optical models for diagnosing surface-atmosphere shortwave interactions, *J. Climate*, in press.

Winton, M., 2003: On the climatic impact of ocean circulation, *J. Climate*, **16**, 2875--2889.

Captions

Table 1: Global mean surface air temperature change and surface albedo feedback (at the surface) averaged over years 1-80 of the 1%/year CO_2 increase experiments; hemispheric ocean and land contributions to SAF.

Figure 1: Impact of perturbing surface and atmospheric optical properties on surface and atmospheric shortwave budgets in 2xCO2 equilibrium experiment with GFDL AM2 (Wm^{-2}). A and S represent the atmospheric and surface optical properties in the control experiments. A' and S' represent the properties in the perturbation (2xCO2) experiments. The vertical arrows show the effect of perturbing atmospheric properties, the horizontal arrows show the effect of perturbing the surface albedo and the diagonal arrows the effect of perturbing both. Top row values are diagnosed using the 4-parameter technique and bottom row (surface) values are diagnosed using the ALL/CLR method.

Figure 2: A: model mean surface air temperature change (K); B: surface albedo feedback ($Wm^{-2}K^{-1}$); C: sensitivity of surface albedo to global surface air temperature (K^{-1}). All are averages over years 1-80 of the 1%/year CO_2 increase experiments. Values within 0.1 $Wm^{-2}K^{-1}$ of zero are not shaded in B. Values within 0.001 K^{-1} of zero are not shaded in C.

Figure 3: Scatter plot of model surface albedo feedback and surface albedo-temperature sensitivity for 1%/year CO_2 increase experiments (global and regional, year 1-80 averages). The line has a slope equal to the model mean $\Delta S/\Delta T_s$ (see equation 1).

Tables

Table 1: Global mean surface air temperature change and surface albedo feedback (at the surface) averaged over years 1-80 of the 1%/year CO_2 increase experiments; hemispheric ocean and land contributions to SAF.

Model	**ΔT (K)**	**SAF ($Wm^{-2}K^{-1}$)**	**SH OCEAN**	**NH OCEAN**	**LAND**
CCCMA CGCM 3.1	1.00	0.29	0.13	0.09	0.07
CNRM CM3	0.77	0.21	0.10	0.07	0.04
GFDL CM2.0	0.92	0.40	0.11	0.12	0.17
GFDL CM2.1	0.78	0.25	0.02	0.10	0.14
GISS MODEL E-H	0.87	0.14	-0.02	0.06	0.10
IAP FGOALS 1.0G	0.82	0.36	0.04	0.22	0.10
MIROC 3.2 HIRES	1.43	0.46	0.15	0.12	0.19
MIROC 3.2 MEDRES	1.05	0.29	0.00	0.11	0.17
MPI ECHAM5	1.13	0.28	0.11	0.10	0.06
NCAR CCSM3.0	0.76	0.27	0.05	0.10	0.12
UKMO HADCM3	1.19	0.32	0.11	0.10	0.11
UKMO HADGEM1	1.02	0.40	0.10	0.16	0.14
Mean (St. Dev.)	0.98 (0.20)	0.30 (0.09)	0.07 (0.05)	0.11 (0.04)	0.12 (0.05)

Figures

Figure 1: Impact of perturbing surface and atmospheric optical properties on surface and atmospheric shortwave budgets in 2xCO2 equilibrium experiment with GFDL AM2 (Wm^{-2}). A and S represent the atmospheric and surface optical properties in the control experiments. A' and S' represent the properties in the perturbation (2xCO2) experiments. The vertical arrows show the effect of perturbing atmospheric properties, the horizontal arrows show the effect of perturbing the surface albedo and the diagonal arrows the effect of perturbing both. Top row values are diagnosed using the 4-parameter technique and bottom row (surface) values are diagnosed using the ALL/CLR method.

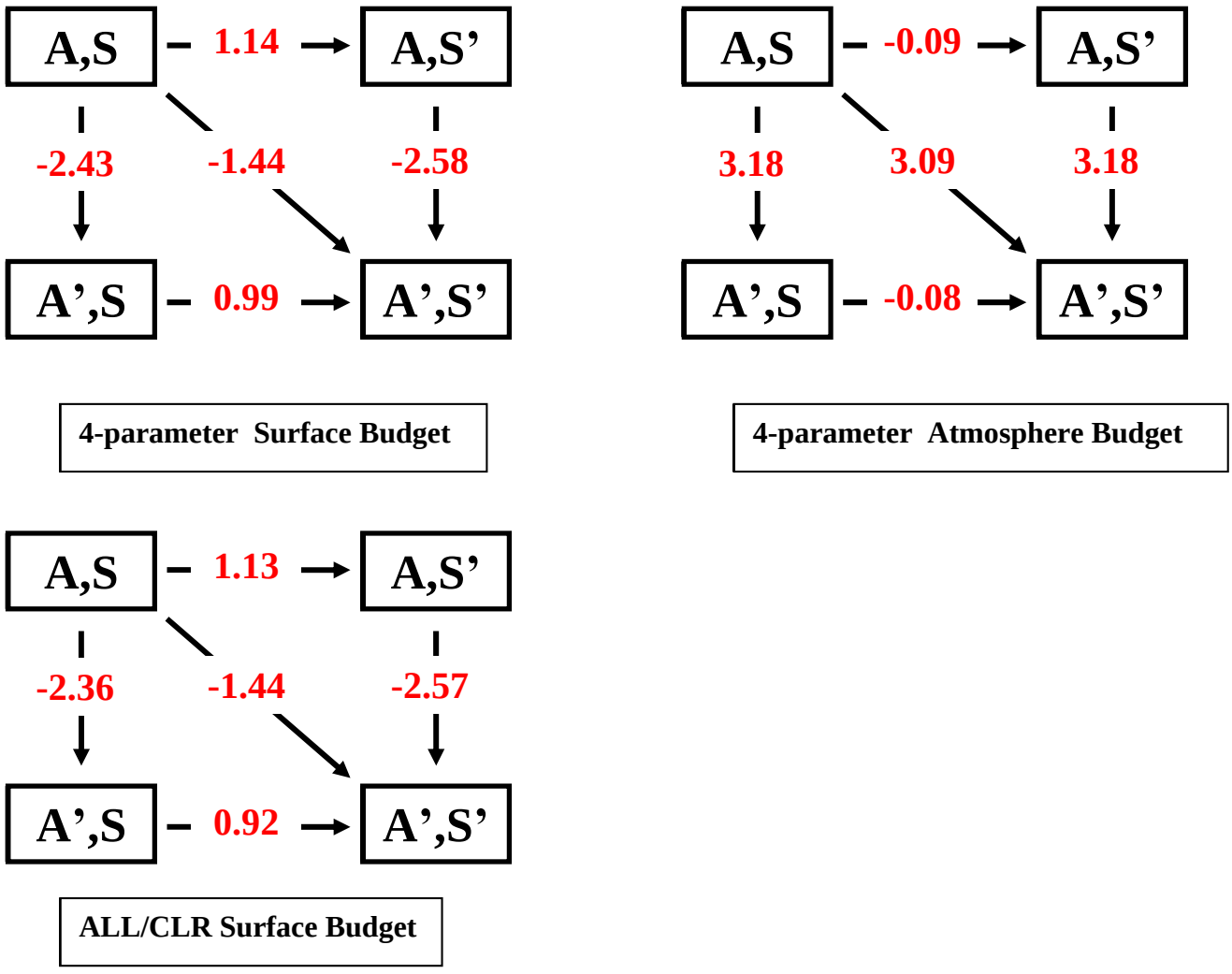

Figure 2: A: model mean surface air temperature change (K); B: surface albedo feedback ($Wm^{-2}K^{-1}$); C: sensitivity of surface albedo to global surface air temperature (K^{-1}). All are averages over years 1-80 of the 1%/year CO_2 increase experiments. Values within 0.1 $Wm^{-2}K^{-1}$ of zero are not shaded in B. Values within 0.001 K^{-1} of zero are not shaded in C.

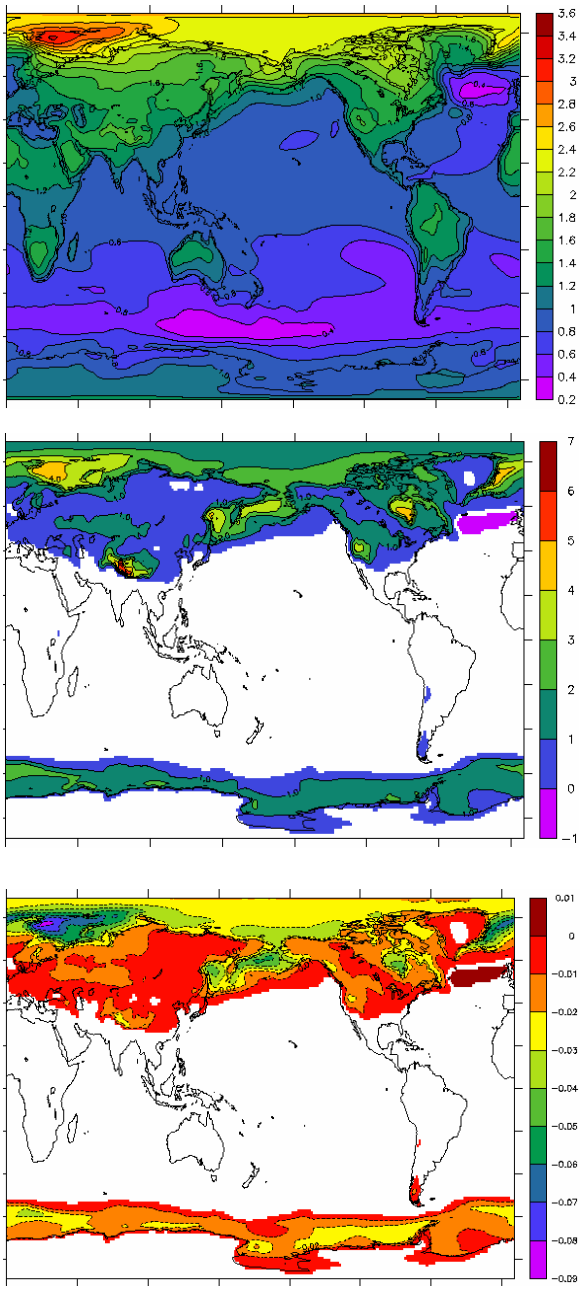

Figure 3: Scatter plot of model surface albedo feedback and surface albedo-temperature sensitivity for 1%/year CO_2 increase experiments (global and regional, year 1-80 averages). The line has a slope equal to the model mean $\Delta S/\Delta\alpha_s$ (see equation 1).